Genetic Control of Developmental Changes Induced by Disruption of Arabidopsis Histone Deacetylase 1 (*AtHD1*) Expression

Lu Tian,*,† Jianlin Wang,* M. Paulus Fong,*,‡ Meng Chen,* Hongbin Cao,§ Stanton B. Gelvin§ and Z. Jeffrey Chen*,†,‡,1

**Department of Soil and Crop Sciences and Intercollegiate Programs in †Genetics and ‡Molecular and Environmental Plant Sciences, Texas A&M University, College Station, Texas 77843-2474 and §Department of Biological Sciences, Purdue University, West Lafayette, Indiana 47907-1392*

Manuscript received April 6, 2003
Accepted for publication May 23, 2003

ABSTRACT

Little is known about the role of genetic and epigenetic control in the spatial and temporal regulation of plant development. Overexpressing antisense *Arabidopsis thaliana HD1* (*AtHD1*) encoding a putative major histone deacetylase induces pleiotropic effects on plant growth and development. It is unclear whether the developmental abnormalities are caused by a defective *AtHD1* or related homologs and are heritable in selfing progeny. We isolated a stable antisense *AtHD1* (CASH) transgenic line and a T-DNA insertion line in exon 2 of *AtHD1*, resulting in a null allele (*athd1-t1*). Both *athd1-t1* and CASH lines display increased levels of histone acetylation and similar developmental abnormalities, which are heritable in the presence of antisense *AtHD1* or in the progeny of homozygous (*athd1-t1/athd1-t1*) plants. Furthermore, when the *athd1-t1/athd1-t1* plants are crossed to wild-type plants, the pleiotropic developmental abnormalities are immediately restored in the F_1 hybrids, which correlates with *AtHD1* expression and reduction of histone H4 Lys12 acetylation. Unlike the situation with the stable code of DNA and histone methylation, developmental changes induced by histone deacetylase defects are immediately reversible, probably through the restoration of a reversible histone acetylation code needed for the normal control of gene regulation and development.

PLANT development is plastic and affected by genetic, epigenetic, and environmental factors. Vegetative and reproductive (inflorescence) development is initiated at shoot apical meristems and/or axillary meristems that can be induced by internal and external signals (Bernier 1986; Walbot 1996; Bleecker and Patterson 1997; Meyerowitz 1997). The molecular mechanisms underlying the plastic nature of plant development are largely unknown. Both genetic and epigenetic changes may contribute to the developmental plasticity of plants (Walbot 1996; Meyerowitz 1997, 2002; Srinivas 2000; Habu *et al.* 2001; Martienssen and Colot 2001).

Epigenetic regulation is a major aspect of gene control by which heritable changes in gene expression occur without an alteration in DNA sequence. Changes in chromatin structure may affect accessibility of promoter elements to the transcriptional machinery and thus affect transcription. Modifications on core histones and their associated covalent bonds are known as the "histone code" (Jenuwein and Allis 2001). Changes in the histone code may facilitate fine tuning of gene expression in response to developmental programs or changes in environmental signals. Disruption of histone deacetylases results in growth and developmental abnormalities and aging in yeast cells (Imai *et al.* 2000). These developmental changes are associated with down- or upregulation of several hundred genes (Bernstein *et al.* 2000; Robyr *et al.* 2002), suggesting that histone deacetylases are key regulators of eukaryotic development. Histone acetylation and deacetylation may also play a role in gene expression and development in animals. For example, mouse histone deacetylase 1 (*HD1*) is a growth factor-inducible gene (Bartl *et al.* 1997). Histone hyperacetylation plays a role in establishing stable states of differential gene activity during gastrulation in Xenopus (Almouzni *et al.* 1994).

The Arabidopsis genome contains 18 putative *HDs* (*HDAs* or *HDACs*) and 12 putative histone acetyltransferases (*HATs*) distributed among all five chromosomes (Arabidopsis Genome Initiative 2000; Pandey *et al.* 2002). There are four classes of histone deacetylases in plants (Lusser *et al.* 2001). First, the RPD3-like protein is the major histone deacetylase in yeast and mammals. Mutations in RPD3 affect ~500 genes in yeast (Bernstein *et al.* 2000; Robyr *et al.* 2002). *Arabidopsis thaliana* HD1 (AtHD1; GenBank accession no. AAB66486), also known as AtHDA19 (Pandey *et al.* 2002), is a putative homolog of yeast RPD3 and the major histone deacetylase (HD1) in humans and mice (Rundlett *et al.* 1996; Taunton *et al.* 1996; Bartl *et al.* 1997; Lusser *et al.*

[1]*Corresponding author:* Molecular Genetics/MS 2474, Department of Soil and Crop Sciences, Texas A&M University, College Station, TX 77843-2474. E-mail: zjchen@tamu.edu

1997). This class consists of at least two isoforms (HD1B-I and -II) in maize embryos (Rossi *et al.* 1998; Lechner *et al.* 2000) and four genes (*HDA6*, *-7*, *-9*, and *-19*) in Arabidopsis. One of the maize genes, *ZmRpd3* or *HD1B-II* (Lechner *et al.* 2000), complements a yeast *rpd3* null mutant (Rossi *et al.* 1998). Second, on the basis of DNA sequences, HDA- and HOS-like HDs are related to RPD3 but have different specific activities in deacetylating histones (Vidal and Gaber 1991; De Rubertis *et al.* 1996; Rundlett *et al.* 1996, 1998). Eight Arabidopsis genes in this category are predicted and some of them may be distinct from other members in this group (Pandey *et al.* 2002). Third, HD2 is a plant-specific histone deacetylase (Lusser *et al.* 1997) localized in the nucleolus. At least two isoforms exist in maize and four genes in Arabidopsis (Lusser *et al.* 1997; Dangl *et al.* 2001). Fourth, a NAD-dependent HD (SIR2-like protein) forms a newly discovered class of HDs (Imai *et al.* 2000; Landry *et al.* 2000). In yeast, the deacetylation by SIR2 is NAD dependent and possibly coupled to ADP ribosylation (Tanner *et al.* 2000). Arabidopsis has two *SIR2*-like genes (Pandey *et al.* 2002).

The role of histone acetylation and deacetylation in plant gene regulation is poorly understood (Verbsky and Richards 2001; Li *et al.* 2002). Transgenic plants treated with propionic or butyric acid, chemical inhibitors of histone deacetylases, display increased levels of DNA methylation and epigenetic variegation (ten Lohuis *et al.* 1995). HC toxin, the host-selective toxin of the maize fungal pathogen *Cochliobolus carbonum*, inhibits histone deacetylases in host plants (Brosch *et al.* 1995). Blocking deacetylation by sodium butyrate or trichostatin A derepresses silent rRNA genes subject to nucleolar dominance (Chen and Pikaard 1997). In a genetic screen for auxin-insensitive mutants, Murfett *et al.* (2001) identified mutagenized plants with enhanced expression of *gusA* and *hptII* transgenes. Further analysis indicated that several of these mutations were in *AtHDA6*, a presumed histone deacetylase, suggesting that this gene is important for transcriptional regulation of the promoters controlling these transgenes. Indeed, *AtHDA6* is required to maintain DNA methylation patterns induced by double-stranded RNA (Aufsatz *et al.* 2002). Overexpression of *OsHDAC1*, a putative histone deacetylase 1 gene in rice, is correlated with the induction of OsHDAC1, increased growth rate, and altered plant morphology (Jang *et al.* 2003). Antisense-mediated downregulation of the Arabidopsis genes *AtHD1* or *AtHD2*, which putatively encode histone deacetylases, results in a variety of abnormal phenotypes in early and late stages of Arabidopsis development (Wu *et al.* 2000a,b; Tian and Chen 2001).

Downregulation of histone deacetylation induces pleiotropic effects on Arabidopsis development (Tian and Chen 2001), suggesting that histone deacetylation directly or indirectly affects the expression of many genes in regulatory networks (Finnegan 2001). However, it is not known whether the abnormal phenotypes observed in the antisense *AtHD1* plants result from the disruption of single gene or related homologs in the *AtHD* multi-gene family. Moreover, it is unclear whether disruption of histone deacetylation induces other epigenetic lesions and whether the induced phenotypic changes are heritable in the absence of the original *AtHD1* defect. Finally, the acetylation code is reversible and dynamic because core histones can be acetylated or deacetylated through the activities of histone acetyltransferases (HATs) or histone deacetylases (HDs, HADs, HDACs) during growth and development (Allfrey *et al.* 1964), whereas the code of DNA and histone methylation is stable because no active demethylation pathway has been identified (Jenuwein and Allis 2001). However, both the stable and reversible codes can be stored in chromatin and propagated through meiosis. Thus, compared to the stable code, the reversible histone acetylation code may contribute differently to gene regulation and development. In this study, we show that defects induced by expressing antisense *AtHD1*, or by T-DNA insertion mutagenesis of *AtHD1*, result in similar developmental pleiotropy. Unlike the situation with *ddm1* (decrease in DNA methylation) mutants, defects in *AtHD1* do not induce cumulative epigenetic lesions after four to five generations of selfing. Furthermore, genetic analyses indicate that disruption of developmental programs, *AtHD1* expression, and histone acetylation is immediately corrected in *AtHD1/athd1-t1* heterozygous plants probably through restoration of the reversible histone acetylation code.

MATERIALS AND METHODS

Plant materials: *C*onstitutive *a*nti*s*ense *h*istone deacetylase (CASH) transgenic plants were described previously (Tian and Chen 2001). All plants were grown in vermiculite mixed with 10% soil in a growth chamber with growth conditions of 22°/18° (day/night) and 16 hr of illumination per day, except as noted otherwise. Seeds from CASH plants were germinated in Murashige/Skoog medium (Sigma, St. Louis) in the presence of 15–50 μg/ml of kanamycin. After 2 weeks the plants were transferred to soil and grown in a growth chamber. The T-DNA insertion line was grown without kanamycin selection except as noted otherwise. All photographs, except those taken with the imaging system in a scanning electron microscope, were taken using a Nikon N-900 digital camera or the CCD system of a Nikon SMZ-100 fluorescence microscope.

Scanning electron microscopy: Scanning electron microscopy was performed using a modified protocol (Murai *et al.* 2002) with a Hitachi s570 scanning electron microscope (Tokyo) at an accelerating voltage of 5–15 kV. Tissue samples were fixed in a solution containing 3% (v/v) formaldehyde/glutaraldehyde and 0.1 M sodium cacodylate buffer (pH 7.4) at room temperature for 13 hr, washed three times with 0.2 M sodium cacodylate buffer (pH 7.4), dehydrated through an ethanol series, critical point dried with CO_2, and sputter coated with gold before viewing by scanning electron microscopy.

Nucleic acid preparation and analysis: RNA and DNA were isolated from at least five leaves of each plant at the same developmental stages as previously described (Chen and Pikaard

1997). For DNA and RNA blot analyses, hybridization was performed following the method of Church and Gilbert (1984). The DNA and RNA blots were washed in 2× SSC and 0.2× SDS at 65° for 30–60 min and hybridization signals were detected using a digital imaging system or exposure to X-ray film or to a PhosphorImager.

PCR-based reverse genetic approach to identify T-DNA insertions in the *AtHD1* gene: We used a PCR-based approach similar to that described by Krysan *et al.* (1996) to identify Arabidopsis (ecotype Ws) mutants containing a T-DNA insertion in or near the *AtHD1* gene. Pooled samples of DNA from 1000, 100, and 20 plants from the Feldmann T-DNA insertion library (Feldmann and Marks 1987; Forsthoefel *et al.* 1992) were successively assayed for insertions, followed by assay of individual plants from the pool of 20 mutant plants. The zygosity of a mutant allele was determined using forward and reverse primers specific to the *AtHD1* gene and one primer specific to the *AtHD1* gene in combination with either a T-DNA left- or right-border primer. *AtHD1* primer sequences were 5′-GCACTAGTGGCGCGCCATGGATACTGGCGGCAA-3′ and 5′-GCAGATCTATTTAAATCGCCTGCTCCGCCCCACC-3′. T-DNA primer sequences were left border, 5′-GATGCACTC GAAATCAGCCAATTTTAGAC-3′; right border, 5′-TCCTTC AATCGTTGCGGTTCTGTCAGTTC-3′. PCR was carried out using 0.5 unit ExTaq (Takara, Berkeley, CA) DNA polymerase with a robocycler (Stratagene, La Jolla, CA) using one cycle of 95° for 5 min, 30–36 cycles of 94° for 40–60 sec, 56° for 1 min, and 72° for 3 min, plus an extension cycle of 72° for 10 min followed by 4° on hold. We used 0.24 μM of each primer and 0.2 mM of each dNTP and either 100 ng DNA (for screening superpools of 1000 plants) or 20 ng DNA (for screening pools of 100, 20, or individual plants) in a 50-μl final reaction volume.

T-DNA junction sequence identification in antisense transgenic lines: T-DNA junction sequences in the CASH lines were identified using a modification of a procedure previously described (Zhou *et al.* 1997). Briefly, 1 μg genomic DNA and 1 μg pBluescript plasmid DNA were separately digested at 37° overnight in a 40-μl reaction containing 10 units of *Pst*I. The digested genomic DNA solution was extracted with phenol/chloroform/isoamylalcohol (25:24:1; Fisher) and precipitated using 2 volumes of ethanol and 1/10 vol of 3 M sodium acetate (pH 5.2). The linear form of pBluescript plasmid was purified using a Gelpure kit (GeneMate; ISC Bioexpress, Kaysville, UT). For DNA ligation, 250 ng of digested genomic DNA and 180 ng of digested pBluescript plasmid DNA were mixed in a 20-μl solution containing 3 units of T4 DNA ligase (Promega, Madison, WI) and incubated at 16° overnight.

Two consecutive PCR reactions were performed using three different primers. T3 primer (5′-AAT TAA CCC TCA CTA AAG GG-3′) was derived from an endogenous sequence of the pBluescript plasmid. TR2 (5′-GAT GGG GAT CAG ATT GTC GTT TC-3′) and TR3 (5′-GTC GTT TCC CGC CTT CAG TTT A-3′) were two nested primers derived from the T-DNA sequence close to the right border. The first PCR reaction was performed using TR2 and T3 primers and 5 μl of ligation solution as template. After purification using a QIAquick PCR purification kit (QIAGEN, Chatsworth, CA), an aliquot of 2 μl PCR product from the first reaction was added to the second PCR reaction containing TR3 and T3 primers. Both PCR reactions were performed for 35 cycles with a program of 30 sec at 94° for denaturation, 30 sec at 52° for annealing, and 3 min at 72° for extension, followed by a final extension at 72° for 8 min. The products of the second PCR amplification were subjected to electrophoresis through a 1.0% agarose gel. The band containing the DNA fragment of interest was excised from the gel and the DNA was purified using a DNA purification kit (GeneMate). The purified PCR product was cloned into the plasmid pGEM T-easy (Promega) and sequenced using an ABI Prism Big Dye terminator cycle sequencing reaction kit (PE Applied Biosystems). The small fragment that appeared in one-step reverse transcriptase (RT)-PCR was cloned into pGEM T-easy (Promega). The plasmid DNA was isolated using a QIAprep spin miniprep kit (QIAGEN) and sequenced.

RT-PCR: RT-PCR was carried out using 500 ng of total RNA prepared from leaf tissues. SuperScript one-step RT-PCR was performed using the Platinum *Taq* system (Invitrogen, San Diego) according to the manufacturer's instructions. The primers used for detecting *AtHD1* transcripts were AtHD1-R, 5′-GCT TAC AAC AAC AAC AAC TCC AGA AAC TT-3′ and AtHD1-F, 5′-AGA AAG CCA GAG AGA GAG AGA GAG ATC AT-3′. For detecting *CYC2b* transcripts, we used the following primers: Cyc2b-F, 5′-TCG GTG TAG AGA TGA AGA GAC AGA-3′ and Cyc2b-R, 5′-GCA ACT AAA CCA ACA AGC TGA AGC-3′.

Strand-specific first-strand cDNAs were synthesized using 500 ng of total RNA and Omniscript reverse transcriptase (QIAGEN). AtHD1-R and AtHD1-F primers were used to synthesize sense and antisense strands of *AtHD1*, respectively. RT was performed at 37° for 60 min and the enzyme was then inactivated by incubation at 93° for 5 min. For antisense *AtHD1* detection, following an initial denaturation step, 35 cycles of PCR were performed using the program of 94° for 30 sec, 57° for 30 sec, and 72° for 1.5 min with a final extension of 10 min at 72°. A 5-μl aliquot of PCR products was resolved by electrophoresis through a 1% agarose gel and subjected to DNA blot analysis. For sense *AtHD1* analysis, PCR was performed using the same conditions as described above, except that 20 cycles were used. Hybridization was performed using a full-length *AtHD1* cDNA as a probe. The actin gene *Act2* (An *et al.* 1996) was used as an internal control for quantification. Relative intensities of individual DNA fragments were measured using a PhosphorImager (Molecular Dynamics, Sunnyvale, CA).

Western blot analysis: Western blot analysis was carried out according to Tian and Chen (2001). In brief, crude protein and histone extracts were prepared and subjected to electrophoresis through 8 and 15% SDS polyacrylamide gels. Immunoblots were prepared and probed with antisera against the N-terminal portion of AtHD1 (Tian and Chen 2001) or with a site-specific antibody against histone H4 Lys12 (Upstate Biotechnology, Lake Placid, NY) and developed by enhanced chemiluminescence (ECL; Amersham, Buckinghamshire, UK).

RESULTS

Isolation of a stable antisense *AtHD1* transgenic plant: AtHD1 is constitutively expressed throughout plant development, although a slightly high level of expression is detected in reproductive tissues. Expressing CASH in transgenic Arabidopsis plants results in the reduction of tetra-acetylated histone H4 and a variety of developmental abnormalities (Tian and Chen 2001). Many lines showed variable phenotypes and deceased in early developmental stages. To understand better the *AtHD1* effects, we isolated a CASH126 line that displayed consistent phenotypes in selfing progeny. CASH126 plants displayed phenotypes in the vegetative and flowering stages in the fourth generation (Figure 1) similar to the "pinhead" phenotype observed in *Argonaute* mutants (Moussian *et al.* 1998; Lynn *et al.* 1999; Morel *et al.* 2002). The plants had defective shoot apical meristems and

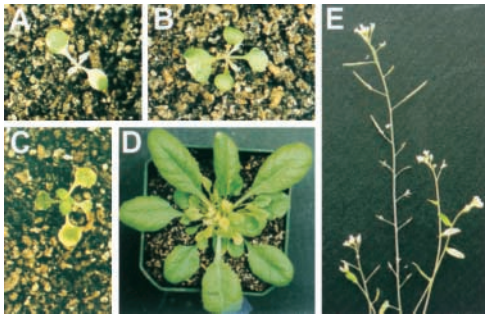

FIGURE 1.—Development and inheritance of phenotypes in a stable CASH126 plant. Only the plants in the fourth generation are shown. (A) A 7-day-old seedling displayed a defective SAM. (B) The defective SAM in the 10-day-old seedling developed a pair of lobed true leaves. (C) A lateral SAM was initiated after 3 weeks. (D) The transition from vegetative to flowering development was delayed. (E) In the flowering stage, the plants display low fertility. About 75% of siliques were small and contained few viable seeds.

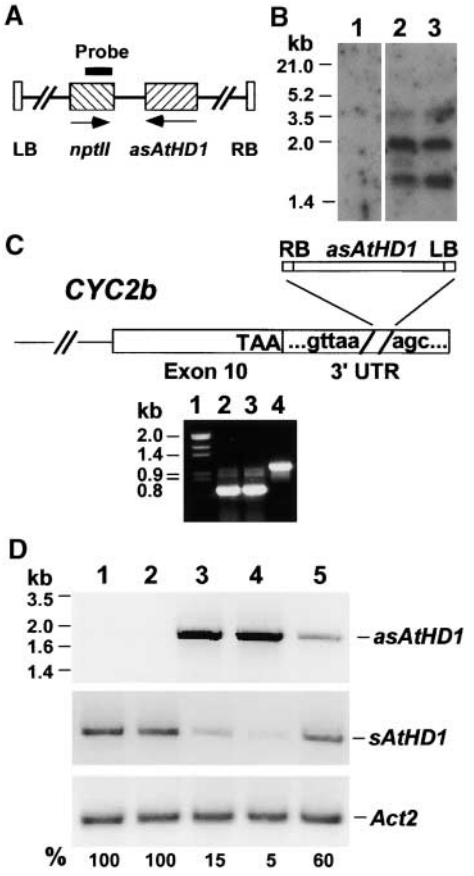

FIGURE 2.—Detection of *AtHD1* transgenes in the genome and expression of the transgene and endogenous *AtHD1* in CASH126 plants. (A) Map of the transgene construction indicating the *nptII* and antisense *AtHD1* (*asAtHD1*) genes located between the left and right T-DNA borders (LB and RB, respectively). (B) DNA blot containing genomic DNA digested with *Bam*HI and *Eco*RI was hybridized with the *nptII* probe. Two copies of the transgene containing *nptII* and *AtHD1* were detected in CASH126 plants (lanes 2 and 3), whereas no transgene was present in the control plant (lane 1). (C) One copy of the *asAtHD1* transgene is inserted into the 3′ untranslated region (UTR) of the *CYC2b* gene, as shown in the top diagram. RT-PCR analysis indicated that *CYC2b* expression was similar in control (lane 2) and CASH126 (lane 3) plants. DNA size markers are shown in lane 1. PCR product amplified from a genomic DNA is shown in lane 4. (D) Strand-specific RT-PCR analysis in CASH126 plants. (Top) *asAtHD1* was highly expressed in CASH 126 plants (lanes 3–5) and undetectable in control plants (ecotype Columbia, lane 1, and ecotype Ws, lane 2). (Middle) RT-PCR and DNA blot analyses were performed to detect the expression levels of sense *AtHD1* (*sAtHD1*). The strand-specific RT-PCR product was resolved by electrophoresis through a 1.0% agarose gel and transferred onto a Hybond-N+ membrane (Amersham Pharmacia). The blot was hybridized with an *AtHD1* full-length cDNA probe. The relative expression levels (%) of sense *AtHD1* (*sAtHD1*) transcripts were estimated using *Act2* as an internal control.

grew slowly *in vitro*. After the plants were transferred to soil, cotyledonary leaves became bleached and yellow. The first pair of true leaves was very small, narrowly elongated, and lacked chlorophyll (Figure 1, A and B). Starting with the second pair of true leaves, leaf development appeared normal except for a delay of the transition from adult vegetative to inflorescence development (Figure 1, C and D). CASH126 plants developed additional true leaves, probably resulting from a developmental transition initiated from axillary meristems. Vegetative development could continue up to 4–5 weeks under long-day (16/8 hr of day/night) conditions. Eventually inflorescences developed from lateral meristems similar to those of wild-type plants. Although some inflorescence branches were sterile (Figure 1E), seeds that could be harvested and germinated and the resulting plants showed developmental abnormalities similar to those observed in plants of previous generations.

One explanation for the abnormal phenotypes in CASH126 plants would be that insertion of the transgenes into the genome disrupted a locus important for plant development, such as a homeotic gene controlling flowering. The endogenous *AtHD1* is a single-copy gene located on chromosome 4 (ARABIDOPSIS GENOME INITIATIVE 2000; TIAN and CHEN 2001). We analyzed the copy number of transgenes in CASH126 plants using DNA blot analysis and detected two fragments of the transgenes (Figure 2, A and B), indicating that these transgenic plants contain two copies of the *AtHD1* transgene. We further used a PCR method (ZHOU *et al.* 1997) to identify the transgene insertion sites in the genome in CASH126. As expected, two fragments were amplified from DNA of transgenic plants. DNA sequencing results indicated that one of the transgene insertion sites was located ~150 bp downstream of the *CYC2b* stop codon of chromosome 4. The insertion did not affect *CYC2b* RNA accumulation; we detected an approximately equal amount of *CYC2b* transcripts in the control and CASH126 plants (Figure 2C). The other insertion site remains unknown, as the sequenced fragment did not match Arabidopsis sequence in the database.

We used strand-specific RT-PCR to determine the ex-

pression levels of antisense and endogenous *AtHD1* genes in transgenic and control plants. Antisense *AtHD1* (*asAtHD1*) transcripts were abundant in each of three CASH126 plants that were derived from single-seed descent, but absent in control plants (Figure 2D, lanes 1 and 2). To determine the expression levels of the endogenous sense *AtHD1* (*sAtHD1*) transcript, we performed a semiquantitative RT-PCR analysis using *Act2* (An *et al.* 1996) as an internal control. *sAtHD1* and *Act2* transcripts were amplified and subjected to DNA blot analysis, and the relative expression ratios of *sAtHD1* and *Act2* transcripts were calculated in control and CASH126 plants. The results indicated that endogenous sense *AtHD1* transcripts were greatly reduced in the CASH126 plants, ranging from 5 to 60% of the level detected in the control plants. It is notable that *sAtHD1* RNA levels were inversely correlated with the amount of *asAtHD1* transcripts (Figure 2D: compare lanes 3–5). Overexpressing the antisense *AtHD1* gene reduced the accumulation of endogenous *AtHD1* transcripts, suggesting that the penetrance of developmental abnormalities is correlated with the level of *sAtHD1* transcript.

A T-DNA insertion in *AtHD1* results in an *AtHD1* null mutation: Phenotypic abnormalities in transgenic plants may fluctuate because of variable levels of transgene expression (Figure 2D). Moreover, although downregulation of *AtHD1* in antisense transgenic plants results in a variety of developmental abnormalities, it is unclear whether these phenotypic changes result from disrupted expression of *AtHD1*. The expression of antisense *AtHD1* may also affect the expression of other genes, because there are several *AtHD1* homologs (Pandey *et al.* 2002). We therefore identified an Arabidopsis (ecotype Ws) mutant line that contains a T-DNA insertion in the *AtHD1* gene (*athd1-t1*; Figure 3A). DNA blot analysis indicated only one T-DNA insertion in the genome (Figure 3B). Using a PCR-based reverse genetic approach (Krysan *et al.* 1996) and DNA sequence analysis, we determined that the T-DNA was inserted into exon 2 of *AtHD1* (Figure 3A). This insertion caused a null mutation of *AtHD1*; no *AtHD1* expression was detected in homozygous insertion lines (lane 7, Figure 3C). Furthermore, Western blot analysis using antibodies against the N terminus of AtHD1 (Tian and Chen 2001) indicated that, in the homozygous mutant line, the level of AtHD1 protein was greatly reduced (Figure 3D, lane 4). Only a small amount of protein (~5% that of the wild type) was detected in homozygous plants, most likely resulting from cross-reaction of the antibodies to other AtHD1 homologs. For example, AtHD1 and AtHD6 share 69 and 84% of amino-acid sequence identity and similarity in the N termini, respectively. Alternatively, the low level of AtHD1 detected could be due to residual expression of *athd1-t1*; however, a different-sized protein would be observed because the T-DNA was inserted in the coding sequence (Figure 3A). Taken together, the data suggest that insertion of T-DNA into exon 2 of *AtHD1* generated an *AtHD1* null mutation.

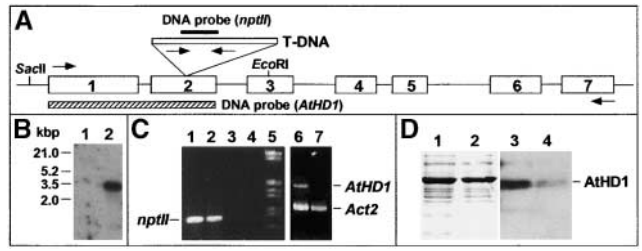

Figure 3.—A null mutation (*athd1-t1*) is generated by T-DNA insertion into the *AtHD1* gene. (A) *AtHD1* contains seven exons. The T-DNA is inserted into exon 2. Primers used in RT-PCR for detecting *AtHD1* expression are shown above the first exon and below the last exon. Primers used to amplify the *nptII* gene in RT-PCR reactions (C) and the *nptII* fragment used for DNA blot analysis (B) are shown below and above the T-DNA diagram, respectively. Striped box indicates the location of the *AtHD1* fragment used for DNA blot analysis in Figure 7. (B) DNA blot analysis shows a single T-DNA insertion in the *athd1-t1* line. (C) RT-PCR analysis indicates that *nptII* gene expression is detected in the *athd1-t1* plants (lanes 1 and 2), but absent in wild-type plants (ecotype Columbia, lane 3; Ws, lane 4). T-DNA insertion produces null alleles in the *AtHD1* locus. *AtHD1* expression was detected in Ws (lane 6) but absent in the *athd1-t1* line (lane 7). *Act2* was amplified as a positive internal control. (D) AtHD1 production is reduced in the *athd1-t1* plants. Crude protein extracts (25 μg) were subjected to electrophoresis though an SDS-polyacrylamide gene and immunoblotted onto Immobilon-P (Millipore, Bedford, MA) or Hybond-ECL (Amersham) membranes. The membrane was probed with antibodies against the N terminus of AtHD1. A band cross-reacting with anti-AtHD1 antibodies in *athd1-t1* plants was reduced to only a trace amount (lane 4) compared to the band detected in the control plant (lane 3). A protein loading control is shown in an 8% SDS-PAGE stained with Coomassie Blue (lanes 1 and 2).

CASH126 and *athd1-t1* plants display similar developmental abnormalities: To determine whether CASH126 and *athd1-t1* plants show similar changes in early developmental stages, we grew them side by side in a growth chamber under short-day conditions (8/16 hr of day/night). The leaves of both CASH126 and *athd1-t1* plants were slightly chlorotic and showed disrupted radial symmetry (Figure 4, A–D), probably resulting from defective shoot apical meristems as previously described (Figure 1). A prominent phenotype was the somewhat left-handed "twist" of the longitudinal axis of rosette leaves in *athd1-t1* plants (Figure 4, B and F). This twist did not occur in other parts of the plants and was different from the previously described "lefty" mutants (Thitamadee *et al.* 2002). This left-handed twist was not obvious in the leaves of CASH126 plants (Figure 4C). However, under close examination, the leaves of CASH126 plants were also twisted (Figure 4G), although the orientation of the distortion was not consistent.

Both wild-type and *AtHD1* disruption lines flowered at approximately the same time, suggesting that vegetative development initiated from axillary meristems had little effect on flowering time under short-day conditions. In a separate experiment we grew plants under long-day

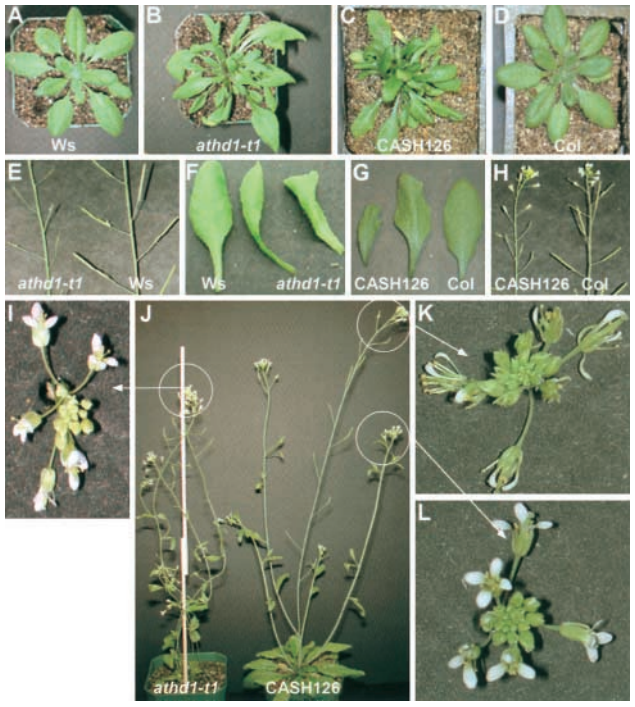

FIGURE 4.—CASH126 and *athd1-t1* plants show similar abnormal developmental phenotypes. CASH126 and *athd1-t1* plants were grown side by side in a growth chamber under short-day (A–H) or long-day (I–L) conditions. (A) Wild-type plant (Ws) 3 weeks after germination. (B) Homozygous *athd1-t1/athd1-t1* plants 3 weeks after germination. (C) CASH126 plants 3 weeks after germination. (D) Wild-type plant (Col, Columbia) 3 weeks after germination. (E) Mature inflorescence branches in *athd1-t1* and Ws. (F) Rosette leaves of Ws and *athd1-t1* plants. (G) Rosette leaves of CASH126 and control plants. (H) Florescence branches of CASH126 and Columbia plants. (I) Enlarged picture of mildly defective flowers in *athd1-t1* plants. (J) Plant morphology of *athd1-t1* and CASH126 plants. (K and L) Enlarged pictures of inflorescence branches showing severely defective flower organs (K) and mildly abnormal flowers (L) of CASH126 plants.

conditions (16/8 hr of day/night). As with the CASH lines, *athd1-t1* lines flowered ~2–5 days late (31.9 ± 1.1 days, $n = 43$) compared to the wild-type plants (28.1 ± 2.3 days, $n = 42$). Although severe phenotypes in the vegetative stage were often observed under short-day conditions (Figure 4, A–D, F, G), similar abnormalities in the reproductive stage were observed under both long- and short-day conditions (Figure 4, E, H, I–L).

CASH126 and *athd1-t1* plants developed abnormal flower structures, including reduced numbers of petals (Figure 4, I, K, and L), split flowers (Figure 4K), and sterility (Figure 4, E and H). The abnormal flower phenotypes in *athd1-t1* plants (Figure 4I) were not as severe as those of CASH126 plants (Figure 4J), but were more uniform. CASH126 lines, however, displayed a range of penetrance in developmental abnormalities, ranging from severe (Figure 4K) to mild (Figure 4L).

CASH126 and *athd1-t1* plants were partially sterile and had low seed set. To investigate the cause of sterility, we examined the flower structures of *athd1-t1* plants using light and scanning electron microscopy. Flower morphology of *athd1-t1* plants was irregular. Many flowers had missing petals and sepals (Figure 5, B, C, and E) compared to the typical "crucifer-shaped" flowers of wild-type plants (Figure 5, A and D). Some flowers had fewer than six stamens, and some of these were fused (Figure 5F). The stamens were short (Figure 5E). As a result, pollen would have difficulty reaching the "tall" stigma. The incompatibility between "impotent" male stamens and tall female stigmas is likely associated with sterility because, compared with wild-type stigmas that were completely covered with pollen grains (Figure 5G), only a few pollen grains could reach the stigmas of homozygous *athd1-t1* plants (arrows in Figure 5H). As a result, siliques of homozygous *athd1-t1* plants were short and contained few seeds (Figure 5, M and O), whereas siliques of wild-type plants were long and contained many fully developed seeds (Figure 5, M and N). Pollen grains of *athd1-t1* plants were apparently normal (Figure 5, K and L). Although structural incompatibility between stigma and stamen is likely related to sterility, we do not rule out other possibilities, such as biological incompatibility between pollen and stigma interactions during pollination in *athd1-t1* plants, which may also cause sterility.

The pleiotropic phenotype resulting from *AtHD1* defects is immediately restored in heterozygous plants and displays Mendelian segregation: The developmental defects of CASH and *athd1-t1/athd1-t1* plants are consistently observed in selfing generations. However, it is unknown whether the phenotypic abnormalities were dependent on the continued deficiency in *AtHD1* expression and core histone acetylation profiles. To address this, we made F_1 hybrids between wild-type (Ws) and homozygous *athd1-t1/athd1-t1* plants (Figure 6A) and examined the phenotypes in the resulting F_1 hybrids and F_2 siblings. In all the F_1 plants examined, most of the developmental abnormalities, including rosette leaf morphology and fertility, were reversed to those of wild-type plants, except that F_1 plants still developed slightly shorter siliques. These results indicate that most of the developmental defects induced by the homozygous mutants are immediately corrected in *AtHD1/athd1-t1* heterozygotes. Indeed, the expression level of *AtHD1* in the heterozygous plants was equal to that of wild-type plants (Figure 6B). Furthermore, the acetylation level of histone H4 Lys12 was increased approximately threefold in the *athd1-t1/athd1-t1* homozygous mutants compared to the wild-type plants (Figure 6C). H4 Lys12 is one of the primary deacetylation sites targeted by RPD3 in yeast (VIDAL and GABER 1991; RUNDLETT *et al.* 1996). The H4 Lys12 level was reversed to that of the wild-type plants in the heterozygous plants, implying that acetylation at some specific sites is responsible for the changes in developmental abnormalities and gene ex-

pression in these plants. In the F_2 progeny, the wild-type and abnormal phenotypes segregated 3:1, cosegregating with the level of *AtHD1* expression in these plants. These data indicate that the developmental abnormalities are dependent on disruption of *AtHD1* expression and of some specific acetylation sites (*e.g.*, H4 Lys12) in the *athd1-t1* lines.

Does *athd1-t1* induce additional epigenetic changes? The *ddm1* mutant induces epigenetic lesions in addition to those observed in the original *ddm1* mutant (Stokes *et al.* 2002). To determine whether *athd1-t1* acts as an epigenetic modulator, we examined phenotypic changes in the plants derived from single-seed descent of one *athd1-t1/athd1-t1* homozygous plant. Consistent with the results in CASH plants, within four generations of selfing we did not observe abnormal phenotypes in these plants in addition to developmental abnormalities observed in the original homozygous plants (Figure 7). Phenotypic abnormalities were less severe under long-day conditions than under short-day conditions, suggesting that the penetrance of phenotypes is dependent on day length. *AtHD1* expression was not detected in the plants after four generations of selfing. These data, together with the immediate restoration of normal development in *AtHD1/athd1-t1* heterozygous plants, suggest that developmental changes induced by disruption of *AtHD1* expression are reversible and dependent on *AtHD1* expression and histone deacetylation.

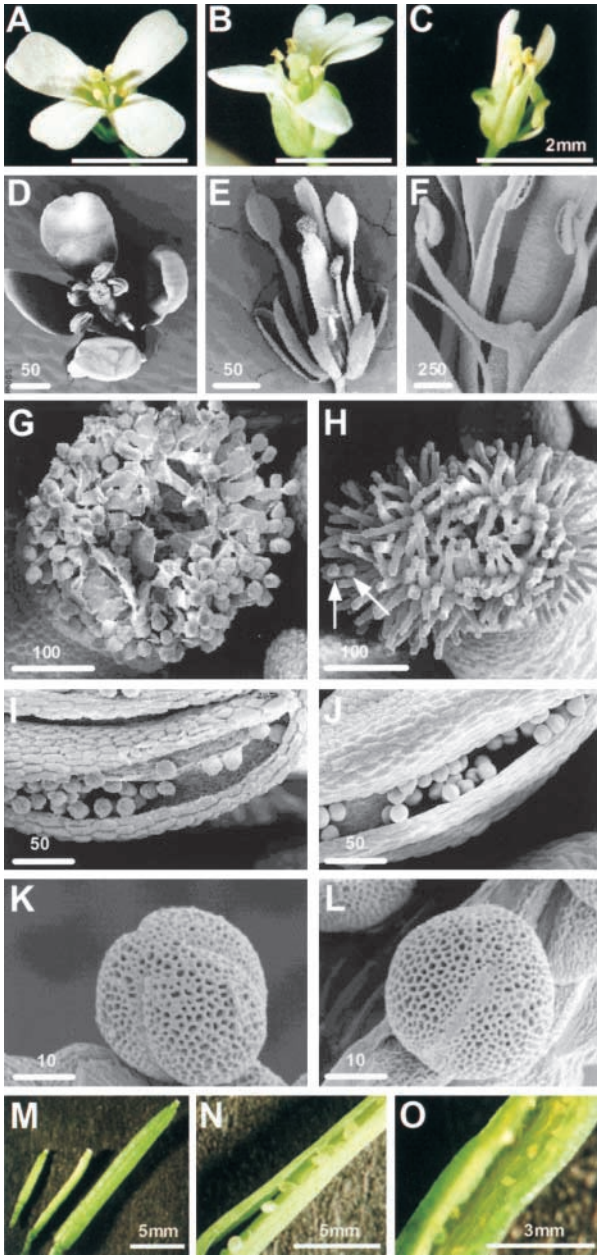

Figure 5.—Abnormal flower development and sterility in *athd1-t1* plants. (A) Wild-type (Ws) plants have a typical "crucifer" flower with four petals, six stamens, and a regular stigma. (B and C) Transformation of the "crucifer" shape into an irregular form in *athd1-t1* plants resulting from fused petals (B) and missing flower parts (C). (D) Normal flower morphology of wild-type plants revealed by scanning electron microscopy. (E and F) Short stamens and missing petals (E) and fused stamens (F) in *athd1-t1* plants. (G) The stigma of the wild-type flower is completely covered with pollen grains. (H) Only a few pollen grains (arrows) are found on the stigma of *athd1-t1* plants. (I and J) Dehisced anthers showing normal pollen development in wild-type (I) and *athd1-t1* (J) plants. (K and L) Pollen grains in Ws (K) and *athd1-t1* (L) anthers. (M). Short and immature siliques (left and middle) developed in *athd1-t1* plants compared to the normal silique in the control (right). (N) Normal seed development in Ws. (O) Abortive seed development in *athd1-t1*.

DISCUSSION

Heritable changes of developmental abnormalities induced by *AtHD1* disruption: Blocking histone deacetylation induces a wide range of developmental changes. The abnormal development includes defective shoot apical meristems (SAM), irregular trichomes and cellular patterns, late flowering, abnormal inflorescences and flowers, and aborted seeds. These developmental abnormalities are stable in the presence of *AtHD1* disruption after four to five generations of selfing. Moreover, a T-DNA insertion into the *AtHD1* gene (*athd1-t1*) results in a mutant line (Ws ecotype) that shows developmental abnormalities similar to those of CASH126 plants (Columbia ecotype), confirming that AtHD1 plays an important role in reprogramming developmental processes. The affected plants develop through initiating axillary meristems and additional changes that ensure the completion of a life cycle, although they have to overcome structural and developmental incompatibilities resulting from irregularly orchestrated patterns and tempos of organogenesis. Histone deacetylation and the resulting effects on gene regulation may contribute to the fundamental and dynamic process of developmental plasticity in plants (Walbot 1996; Meyer-

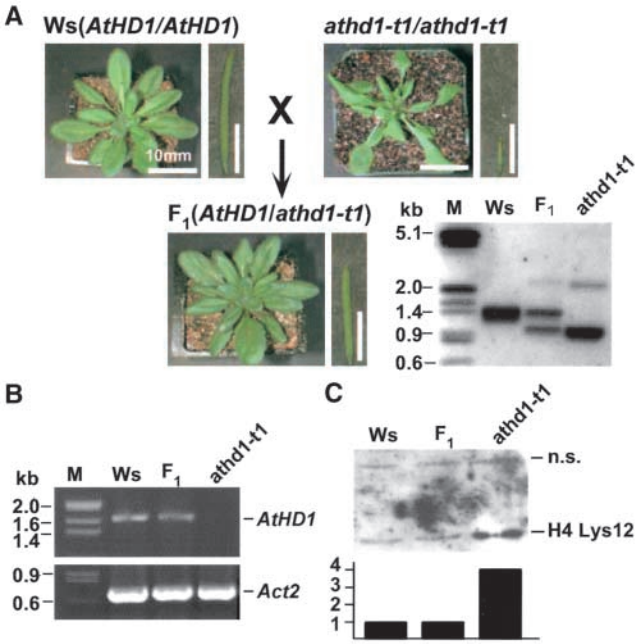

FIGURE 6.—(A) Developmental abnormalities in rosette leaves and siliques of *athd1-t1/athd1-t1* homozygous plants were restored in F_1 (*AtHD1/athd1-t1*) progeny. The F_1 hybrid, heterozygous for the *athd1-t1* locus, was generated by crossing a wild-type Ws plant with a homozygous *athd1-t1* plant. (Right) Genomic DNA was digested with *Eco*RI and *Sac*II, subjected to electrophoresis through a 1% agarose gel, and blotted onto a Hybond + membrane. The blot was hybridized with a DNA fragment containing exons 1 and 2 of *AtHD1* (see Figure 3A). The F_1 plant contained a normal *AtHD1* allele and an *athd1-t1* allele. (B) Equal quantities of *AtHD1* transcripts were detected by RT-PCR in the F_1 and Ws plants, but no *AtHD1* transcript was detected in the *athd1-t1/athd1-t1* homozygous plants. RT-PCR amplification of *Act2* was used as an internal control. (C) Western blot indicates that histone H4 Lys12 acetylation is increased in the homozygous *athd1-t1* plants. Hybridization intensities of a nonspecific (n.s.) protein detected by the anti-H4 Lys12 antibody were used as internal controls to calculate the relative ratio of H4 Lys12 acetylation accumulation, which is shown in a histogram below the Western blot.

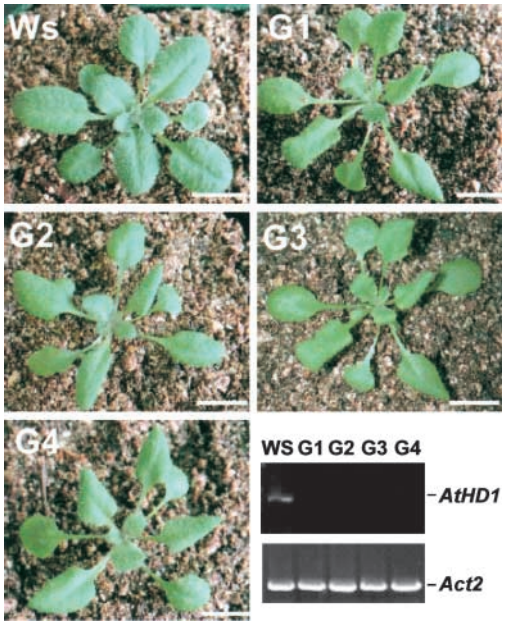

FIGURE 7.—*athd1-t1/athd1-t1* plants showed constant developmental abnormalities during four generations (G_1–G_4) of selfing. The plants were grown side by side in the same growth chamber. No *AtHD1* expression was detected by RT-PCR in the homozygous *athd1-t1/athd1-t1* plants obtained in four generations of selfing.

owitz 1997). Disruption of AtHDs may directly affect expression of genes such as *superman* (Tian and Chen 2001) in specific developmental stages. Alternatively, the disruption may induce a series of changes in regulatory networks. Complex phenotypes such as defective apical shoot meristems and abnormal flowers could be some of these pleiotropic effects. It will be interesting to identify target genes whose expression is affected in the *athd1-t1* and antisense *AtHD1* transgenic lines.

Developmental abnormalities induced by disruption of histone deacetylation are different from those induced by DNA methylation defects (Vongs *et al.* 1993; Finnegan *et al.* 1996; Ronemus *et al.* 1996; Gendrel *et al.* 2002; Stokes and Richards 2002). First, the abnormal development in the *athd1-t1* homozygous plants can be immediately corrected in the heterozygous state. Second, no additional visual abnormalities accumulate in the selfing progeny of *athd1-t1/athd1-t1* homozygous plants. The data suggest that the dynamic and reversible process of acetylation and deacetylation provides a spatial and temporal code for gene activation and silencing. Consistent with this hypothesis, histone deacetylation may affect the expression of genes in response to environmental (*e.g.*, light, day length) and developmental (*e.g.*, homeotic genes) changes. Indeed, both antisense *AtHD1* transgenic and *athd-t1* homozygous lines show variable flowering time and severity of developmental abnormalities under short- and long-day conditions.

AtHD1 is a member of a multi-gene family that may diverge in functions. For example, AtHD6, a RPD3-like homolog, is involved in the release of transgene silencing (Murfett *et al.* 2001) and is associated with the maintenance of DNA methylation patterns of transgenes (Aufsatz *et al.* 2002). However, recessive mutations in *AtHDA6* do not induce visible abnormal phenotypes (Murfett *et al.* 2001). Antisense *AtHD2* lines (Wu *et al.* 2000a,b) show less severe developmental abnormalities than antisense *AtHD1* lines do (Tian and Chen 2001). Significantly, although histone deacetylases are encoded by a multi-gene family and share sequence homology (Pandey *et al.* 2002), other AtHD homologs cannot compensate for the loss of AtHD1 activity in the *athd1-t1* lines, suggesting that *AtHD1* is a key member of the histone deacetylase gene family. Unlike the tetra-acetylated histone H4 induced by overexpressing anti-

sense *AtHD1* (Tian and Chen 2001), hyper-acetylation of core histones in the *athd1-t1* line is restricted to a specific set of lysine residues including H4 Lys12. These data suggest that specific patterns of histone acetylation may be established by AtHD1, consequently controlling the expression of a subset of genes during development.

The role of a histone code in genetic and epigenetic regulation: Chromatin-based gene regulation in eukaryotes is controlled by a chromatin code (Jenuwein and Allis 2001) that can be further classified as stable or reversible. The stable code includes DNA and histone methylation (Richards and Elgin 2002). Once the stable code is established, it is difficult to alter unless through a reset of developmental programming during meiosis, because no active demethylation pathway has been identified (Jenuwein and Allis 2001; Li 2002; Richards and Elgin 2002). As a result, changing a stable code results in epigenetic inheritance or variation (Stokes *et al.* 2002; Stokes and Richards 2002). Moreover, alteration in the stable code may serve as an epigenetic "modulator" that induces changes at other loci, independent of the original chromatin conformation. Indeed, in the *ddm1* genetic background, epigenetic lesions are induced in a genomic region containing multiple repeats associated with disease resistance genes, presumably because they are vulnerable in response to changes in DNA methylation (Stokes and Richards 2002). Moreover, these epialleles may be affected not only by demethylation, but also by allelic interactions among loci or within a locus (Stokes *et al.* 2002), a phenomenon similar to meiotic transvection (Aramayo and Metzenberg 1996) or paramutation (Hollick *et al.* 1997). Methylation-associated epialleles have also been reported in mutants with defective flower structure (*e.g.*, SUPERMAN) or a delay in flowering time (*e.g.*, FWA), which may result from aberrant DNA methylation patterns (Jacobsen and Meyerowitz 1997; Kakutani 1997; Soppe *et al.* 2000).

The reversible code (*e.g.*, histone acetylation and deacetylation) is heritable (Jenuwein and Allis 2001) but the action of the code is dependent on the respective biochemical activities that set the code. The code is dynamic and reversible during any developmental stage and is independent of meiosis. Although the connection between a specific acetylation code and gene regulation remains to be elucidated, the heritable and reversible nature of developmental abnormalities observed in *AtHD1* disruption lines is likely associated with changes in histone acetylation (*e.g.*, H4 Lys12 acetylation) and methylation. It is conceivable that under normal conditions, genes, including homeotic genes (*e.g.*, *superman*; Tian and Chen 2001) responsible for plant development, may be controlled by the reversible code of acetylation and deacetylation. However, the acetylation code is reversible and dependent on histone deacetylases or other factors in the chromatin control. As soon as the proper code is restored, controls of regulatory networks and developmental programs return to normal, independent of reprogramming through meiosis. The concept of a stable or reversible code is also supported by the results obtained from a recent study indicating that the loss of histone H4 Lys16 acetylation in *ddm1* homozygous plants is compensated in *DDM1/ddm1* heterozygous plants, whereas DNA and histone H3 Lys9 methylation remain unchanged (Soppe *et al.* 2002).

The relationship between reversible and stable codes is largely unknown. Acetylation and deacetylation may act on active or inactive chromatin as a competitor for histone methylation sites (Jenuwein and Allis 2001). For example, histone acetyltransferases and methyltransferases may compete for histone H3 Lys9 to establish an active or inactive form of chromatin (Jenuwein and Allis 2001; Litt *et al.* 2001). Histone deacetylation and DNA methylation may also be interdependent (Selker 1998; Soppe *et al.* 2002). Moreover, a putative histone deactylase (AtHDA6) is needed to enhance DNA methylation induced by double-stranded RNA (Aufsatz *et al.* 2002). Finally, some DNA methyltransferases (*e.g.*, CMT) or histone deacetylases (*e.g.*, HD2) were identified only in plants (Lusser *et al.* 1997, 2001; Henikoff and Comai 1998; Lindroth *et al.* 2001), suggesting that plants may control gene regulation via both general and unique chromatin pathways. It will be interesting to test how the reversible code of histone acetylation controlled by AtHD1 interacts with the biochemically stable code of DNA and histone methylation and affects the plastic nature of plant development.

We thank Eric J. Richards for insightful discussions and Gary E. Hart and Karel Riha for critical suggestions on improving the manuscript, Joe Wang for assistance in photography, Hyeon-Se Lee and Jenny Lee for helpful discussions, and Mike Pendleton in the Microscopy and Imaging Center at Texas A&M University for providing excellent technical services. Work in S.B.G.'s laboratory was supported by grants (99-75715 and 99-75930) from the National Science Foundation Plant Genome Research Program. Research in the Chen laboratory was supported by a grant (00-77774) from the National Science Foundation Plant Genome Research program and the Texas Agricultural Experiment Station.

LITERATURE CITED

Allfrey, V. G., R. Faulkner and A. E. Mirsky, 1964 Acetylation and methylation of histones and their possible role in regulation of RNA synthesis. Proc. Natl. Acad. Sci. USA **51:** 786–794.

Almouzni, G., S. Khochbin, S. Dimitrov and A. P. Wolffe, 1994 Histone acetylation influences both gene expression and development of *Xenopus laevis*. Dev. Biol. **165:** 654–669.

An, Y. Q., J. M. McDowell, S. Huang, E. C. McKinney, S. Chambliss *et al.*, 1996 Strong, constitutive expression of the *Arabidopsis* Act2/Act8 actin subclass in vegetative tissues. Plant J. **10:** 107–121.

Arabidopsis Genome Initiative, 2000 Analysis of the genome sequence of the flowering plant *Arabidopsis thaliana*. Nature **408:** 796–815.

Aramayo, R., and R. L. Metzenberg, 1996 Meiotic transvection in fungi. Cell **86:** 103–113.

Aufsatz, W., M. F. Mette, J. Van Der Winden, M. Matzke and A. J. Matzke, 2002 HDA6, a putative histone deacetylase needed to enhance DNA methylation induced by double-stranded RNA. EMBO J. **21:** 6832–6841.

Bartl, S., J. Taplick, G. Lagger, H. Khier, K. Kuchler *et al.*, 1997 Identification of mouse histone deacetylase 1 as a growth factor-inducible gene. Mol. Cell. Biol. **17:** 5033–5043.

Bernier, G., 1986 The flowering process as an example of plastic development. Symp. Soc. Exp. Biol. **40:** 257–286.

Bernstein, B. E., J. K. Tong and S. L. Schreiber, 2000 Genomewide studies of histone deacetylase function in yeast. Proc. Natl. Acad. Sci. USA **97:** 13708–13713.

Bleecker, A. B., and S. E. Patterson, 1997 Last exit: senescence, abscission, and meristem arrest in *Arabidopsis*. Plant Cell **9:** 1169–1179.

Brosch, G., R. Ransom, T. Lechner, J. D. Walton and P. Loidl, 1995 Inhibition of maize histone deacetylases by HC toxin, the host-selective toxin of *Cochliobolus carbonum*. Plant Cell **7:** 1941–1950.

Chen, Z. J., and C. S. Pikaard, 1997 Epigenetic silencing of RNA polymerase I transcription: a role for DNA methylation and histone modification in nucleolar dominance. Genes Dev. **11:** 2124–2136.

Church, G. M., and W. Gilbert, 1984 Genomic sequencing. Proc. Natl. Acad. Sci. USA **81:** 1991–1995.

Dangl, M., G. Brosch, H. Haas, P. Loidl and A. Lusser, 2001 Comparative analysis of HD2 type histone deacetylases in higher plants. Planta **213:** 280–285.

De Rubertis, F., D. Kadosh, S. Henchoz, D. Pauli, G. Reuter *et al.*, 1996 The histone deacetylase RPD3 counteracts genomic silencing in *Drosophila* and yeast. Nature **384:** 589–591.

Feldmann, K. A., and M. D. Marks, 1987 *Agrobacterium*-mediated transformation of germinating seeds of *Arabidopsis thaliana*: a non-tissue culture approach. Mol. Gen. Genet. **208:** 1–9.

Finnegan, E. J., 2001 Is plant gene expression regulated globally? Trends Genet. **17:** 361–365.

Finnegan, E. J., W. J. Peacock and E. S. Dennis, 1996 Reduced DNA methylation in *Arabidopsis thaliana* results in abnormal plant development. Proc. Natl. Acad. Sci. USA **93:** 8449–8454.

Forsthoefel, N. R., Y. Wu, B. Schulz, M. J. Bennett and K. A. Feldmann, 1992 T-DNA insertion mutagenesis in *Arabidopsis*: prospects and perspectives. Aust J. Plant Physiol. **19:** 353–366.

Gendrel, A. V., Z. Lippman, C. Yordan, V. Colot and R. A. Martienssen, 2002 Dependence of heterochromatic histone H3 methylation patterns on the Arabidopsis gene DDM1. Science **297:** 1871–1873.

Habu, Y., T. Kakutani and J. Paszkowski, 2001 Epigenetic developmental mechanisms in plants: molecules and targets of plant epigenetic regulation. Curr. Opin. Genet. Dev. **11:** 215–220.

Henikoff, S., and L. Comai, 1998 A DNA methyltransferase homolog with a chromodomain exists in multiple polymorphic forms in Arabidopsis. Genetics **149:** 307–318.

Hollick, J. B., J. E. Dorweiler and V. L. Chandler, 1997 Paramutation and related allelic interactions. Trends Genet. **13:** 302–308.

Imai, S., C. M. Armstrong, M. Kaeberlein and L. Guarente, 2000 Transcriptional silencing and longevity protein Sir2 is an NAD-dependent histone deacetylase. Nature **403:** 795–800.

Jacobsen, S. E., and E. M. Meyerowitz, 1997 Hypermethylated *SUPERMAN* epigenetic alleles in *Arabidopsis*. Science **277:** 1100–1103.

Jang, I. C., Y. M. Pahk, S. I. Song, H. J. Kwon, B. H. Nahm *et al.*, 2003 Structure and expression of the rice class-I type histone deacetylase genes OsHDAC1–3: OsHDAC1 overexpression in transgenic plants leads to increased growth rate and altered architecture. Plant J. **33:** 531–541.

Jenuwein, T., and C. D. Allis, 2001 Translating the histone code. Science **293:** 1074–1080.

Kakutani, T., 1997 Genetic characterization of late-flowering traits induced by DNA hypomethylation mutation in *Arabidopsis thaliana*. Plant J. **12:** 1447–1451.

Krysan, P. J., J. C. Young, F. Tax and M. R. Sussman, 1996 Identification of transferred DNA insertions within *Arabidopsis* genes involved in signal transduction and ion transport. Proc. Natl. Acad. Sci. USA **93:** 8145–8150.

Landry, J., A. Sutton, S. T. Tafrov, R. C. Heller, J. Stebbins *et al.*, 2000 The silencing protein SIR2 and its homologs are NAD-dependent protein deacetylases. Proc. Natl. Acad. Sci. USA **97:** 5807–5811.

Lechner, T., A. Lusser, A. Pipal, G. Brosch, A. Loidl *et al.*, 2000 RPD3-type histone deacetylases in maize embryos. Biochemistry **39:** 1683–1692.

Li, E., 2002 Chromatin modification and epigenetic reprogramming in mammalian development. Nat. Rev. Genet. **3:** 662–673.

Li, G., T. C. Hall and R. Holmes-Davis, 2002 Plant chromatin: development and gene control. Bioessays **24:** 234–243.

Lindroth, A. M., X. Cao, J. P. Jackson, D. Zilberman, C. M. McCallum *et al.*, 2001 Requirement of CHROMOMETHYLASE3 for maintenance of CpXpG methylation. Science **292:** 2077–2080.

Litt, M. D., M. Simpson, M. Gaszner, C. D. Allis and G. Felsenfeld, 2001 Correlation between histone lysine methylation and developmental changes at the chicken beta-globin locus. Science **293:** 2453–2455.

Lusser, A., G. Brosch, A. Loidl, H. Haas and P. Loidl, 1997 Identification of maize histone deacetylase HD2 as an acidic nucleolar phosphoprotein. Science **277:** 88–91.

Lusser, A., D. Kolle and P. Loidl, 2001 Histone acetylation: lessons from the plant kingdom. Trends Plant Sci. **6:** 59–65.

Lynn, K., A. Fernandez, M. Aida, J. Sedbrook, M. Tasaka *et al.*, 1999 The PINHEAD/ZWILLE gene acts pleiotropically in Arabidopsis development and has overlapping functions with the ARGONAUTE1 gene. Development **126:** 469–481.

Martienssen, R., and V. Colot, 2001 DNA methylation and epigenetic inheritance in plants and filamentous fungi. Science **293:** 1070–1074.

Meyerowitz, E. M., 1997 Genetic control of cell division patterns in developing plants. Cell **88:** 299–308.

Meyerowitz, E. M., 2002 Plants compared to animals: the broadest comparative study of development. Science **295:** 1482–1485.

Morel, J. B., C. Godon, P. Mourrain, C. Beclin, S. Boutet *et al.*, 2002 Fertile hypomorphic ARGONAUTE (ago1) mutants impaired in post-transcriptional gene silencing and virus resistance. Plant Cell **14:** 629–639.

Moussian, B., H. Schoof, A. Haecker, G. Jurgens and T. Laux, 1998 Role of the ZWILLE gene in the regulation of central shoot meristem cell fate during Arabidopsis embryogenesis. EMBO J. **17:** 1799–1809.

Murai, K., S. Takumi, H. Koga and Y. Ogihara, 2002 Pistillody, homoeotic transformation of stamens into pistil-like structures, caused by nuclear-cytoplasm interaction in wheat. Plant J. **29:** 169–181.

Murfett, J., X. J. Wang, G. Hagen and T. J. Guilfoyle, 2001 Identification of *Arabidopsis* histone deacetylase hda6 mutants that affect transgene expression. Plant Cell **13:** 1047–1061.

Pandey, R., A. Muller, C. A. Napoli, D. A. Selinger, C. S. Pikaard *et al.*, 2002 Analysis of histone acetyltransferase and histone deacetylase families of *Arabidopsis thaliana* suggests functional diversification of chromatin modification among multicellular eukaryotes. Nucleic Acids Res. **30:** 5036–5055.

Richards, E. J., and S. C. Elgin, 2002 Epigenetic codes for heterochromatin formation and silencing: rounding up the usual suspects. Cell **108:** 489–500.

Robyr, D., Y. Suka, I. Xenarios, S. K. Kurdistani, A. Wang *et al.*, 2002 Microarray deacetylation maps determine genome-wide functions for yeast histone deacetylases. Cell **109:** 437–446.

Ronemus, M. J., M. Galbiati, C. Ticknor, J. Chen and S. L. Dellaporta, 1996 Demethylation-induced developmental pleiotropy in *Arabidopsis*. Science **273:** 654–657.

Rossi, V., H. Hartings and M. Motto, 1998 Identification and characterisation of an *RPD3* homologue from maize (*Zea mays* L.) that is able to complement an *rpd3* null mutant of *Saccharomyces cerevisiae*. Mol. Gen. Genet. **258:** 288–296.

Rundlett, S. E., A. A. Carmen, R. Kobayashi, S. Bavykin, B. M. Turner *et al.*, 1996 HDA1 and RPD3 are members of distinct yeast histone deacetylase complexes that regulate silencing and transcription. Proc. Natl. Acad. Sci. USA **93:** 14503–14508.

Rundlett, S. E., A. A. Carmen, N. Suka, B. M. Turner and M. Grunstein, 1998 Transcriptional repression by UME6 involves deacetylation of lysine 5 of histone H4 by RPD3. Nature **392:** 831–835.

Selker, E. U., 1998 Trichostatin A causes selective loss of DNA methylation in Neurospora. Proc. Natl. Acad. Sci. USA **95:** 9430–9435.

Soppe, W. J., S. E. Jacobsen, C. Alonso-Blanco, J. P. Jackson, T. Kakutani *et al.*, 2000 The late flowering phenotype of *fwa* mutants is caused by gain-of-function epigenetic alleles of a homeodomain gene. Mol. Cell **6:** 791–802.

Soppe, W. J. J., Z. Jasencakova, A. Houben, T. Kakutani, A. Meister *et al.*, 2002 DNA methylation controls histone H3 lysine 9 methylation and heterochromatin assembly in *Arabidopsis*. EMBO J. **21:** 6549–6559.

Srinivas, S., 2000 Development: nature and nurture. J. Cell Sci. **113:** 3549–3550.

Stokes, T. L., and E. J. Richards, 2002 Induced instability of two Arabidopsis constitutive pathogen-response alleles. Proc. Natl. Acad. Sci. USA **99:** 7792–7796.

Stokes, T. L., B. N. Kunkel and E. J. Richards, 2002 Epigenetic variation in *Arabidopsis* disease resistance. Genes Dev. **16:** 171–182.

Tanner, K. G., J. Landry, R. Sternglanz and J. M. Denu, 2000 Silent information regulator 2 family of NAD-dependent histone/protein deacetylases generates a unique product, 1-O-acetyl-ADP-ribose. Proc. Natl. Acad. Sci. USA **97:** 14178–14182.

Taunton, J., C. A. Hassig and S. L. Schreiber, 1996 A mammalian histone deacetylase related to the yeast transcriptional regulator Rpd3p. Science **272:** 408–411.

ten Lohuis, M., H. Galliano, I. Heidmann and P. Meyer, 1995 Treatment with propionic and butyric acid enhances expression variegation and promoter methylation in plant transgenes. Biol. Chem. Hoppe Seyler **376:** 311–320.

Thitamadee, S., K. Tuchihara and T. Hashimoto, 2002 Microtubule basis for left-handed helical growth in *Arabidopsis*. Nature **417:** 193–196.

Tian, L., and Z. J. Chen, 2001 Blocking histone deacetylation in *Arabidopsis* induces pleiotropic effects on plant gene regulation and development. Proc. Natl. Acad. Sci. USA **98:** 200–205.

Verbsky, M. L., and E. J. Richards, 2001 Chromatin remodeling in plants. Curr. Opin. Plant Biol. **4:** 494–500.

Vidal, M., and R. F. Gaber, 1991 RPD3 encodes a second factor required to achieve maximum positive and negative transcriptional states in *Saccharomyces cerevisiae*. Mol. Cell. Biol. **11:** 6317–6327.

Vongs, A., T. Kakutani, R. A. Martienssen and E. J. Richards, 1993 *Arabidopsis thaliana* DNA methylation mutants. Science **260:** 1926–1928.

Walbot, V., 1996 Sources and consequences of phenotypic and genotypic plasticity in flowering plants. Trends Plant Sci. **1:** 27–32.

Wu, K., K. Malik, L. Tian, D. Brown and B. Miki, 2000a Functional analysis of a RPD3 histone deacetylase homologue in *Arabidopsis thaliana*. Plant Mol. Biol. **44:** 167–176.

Wu, K., L. Tian, K. Malik, D. Brown and B. Miki, 2000b Functional analysis of HD2 histone deacetylase homologues in *Arabidopsis thaliana*. Plant J. **22:** 19–27.

Zhou, Y. X., R. J. Newton and J. H. Gould, 1997 A simple method for identifying plant/T-DNA junction sequences resulting from *Agrobacterium*-mediated DNA transformation. Plant Mol. Biol. Rep. **15:** 246–254.

Communicating editor: J. A. Birchler